Support Information

Enhanced oxygen evolution catalytic activity of NiS_2 by coupling with ferrous phosphite and phosphide

Jie Yu, [ab] *Tao Zhang,* [a] *Changchang Xing,* [ab] *Xuejiao Li,* [ab] *Xinyang Li,* [a] *Bo Wu*[c] *and Yue Li* *[a]

a Key Laboratory of Materials Physics, Institute of Solid State Physics, HFIPS, Chinese Academy of Sciences, Hefei 230031, China

b University of Science and Technology of China, Hefei, 230026, P. R. China

c State Key Laboratory of Environment-friendly Energy Materials, Southwest University of Science and Technology, Mianyang, 621010, China

*Email: yueli@issp.ac.cn

EXPERIMENTAL SECTION

ECSA calculation: The value of electrochemically active surface area (ECSA) of the electrocatalysts was calculated using the following equation:

$$ECSA = C_{dl} / C_s \times S$$

where C_{dl} was given by the slope of the linear relationship between capacitive currents (j) and scan rate (ν) in non-Faradaic region ($C_{dl} = j / \nu$), C_s is a general surface specific capacitance (0.040 mF cm^2 in 1 M KOH solution)[1], S is the geometric surface area of work electrode (1 cm^2 in this work).

TOF calculation: The value of turnover frequency (TOF) of the electrocatalysts was calculated using the follow equation:

$$TOF = (J \times A) / (4 \times F \times n)$$

where J is the current density at a given overpotential, A is the geometric surface area of work electrode (1 cm^2 in this work), F is the Faradic constant (96485 C mol^{-1}) and n is the number of moles of all metals (Ni and Fe in this work) in the electrode given by ICP.

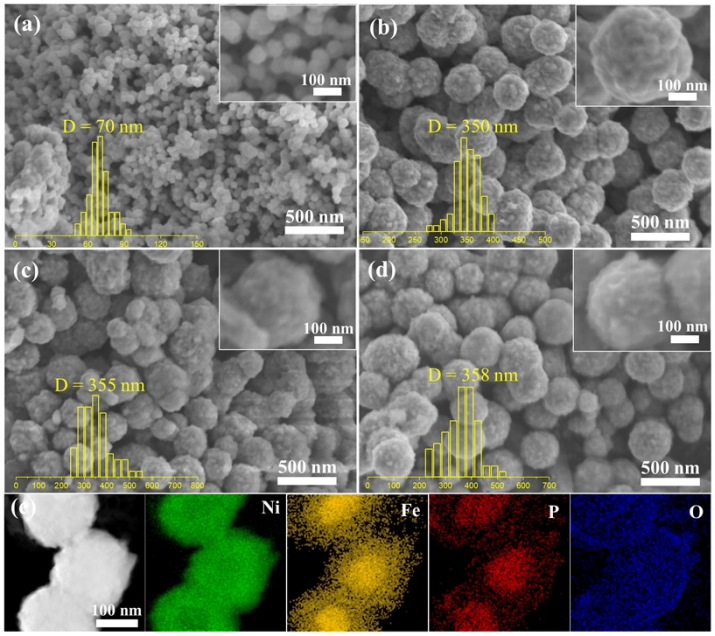

Figure S1. SEM images and particle size distribution of (a) Ni, (b) Ni/$Fe_{0.2}$-HPO, (c) Ni/$Fe_{0.8}$-HPO and (d) Ni/$Fe_{1.0}$-HPO; (e) Energy-dispersive X-ray spectroscopy elemental mapping of Ni/$Fe_{0.4}$-HPO.

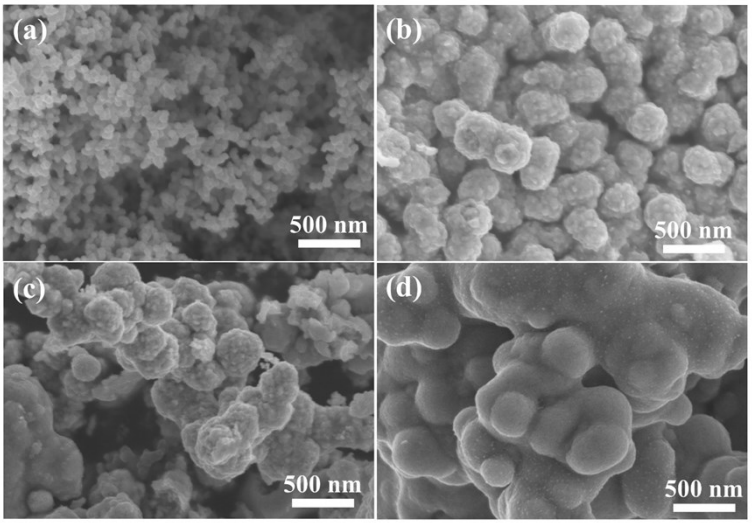

Figure S2. SEM images of (a) NiS_2, (b) NiS_2/$Fe_{0.2}$-P, (c) NiS_2/$Fe_{0.8}$-P and (d) NiS_2/$Fe_{1.0}$-P.

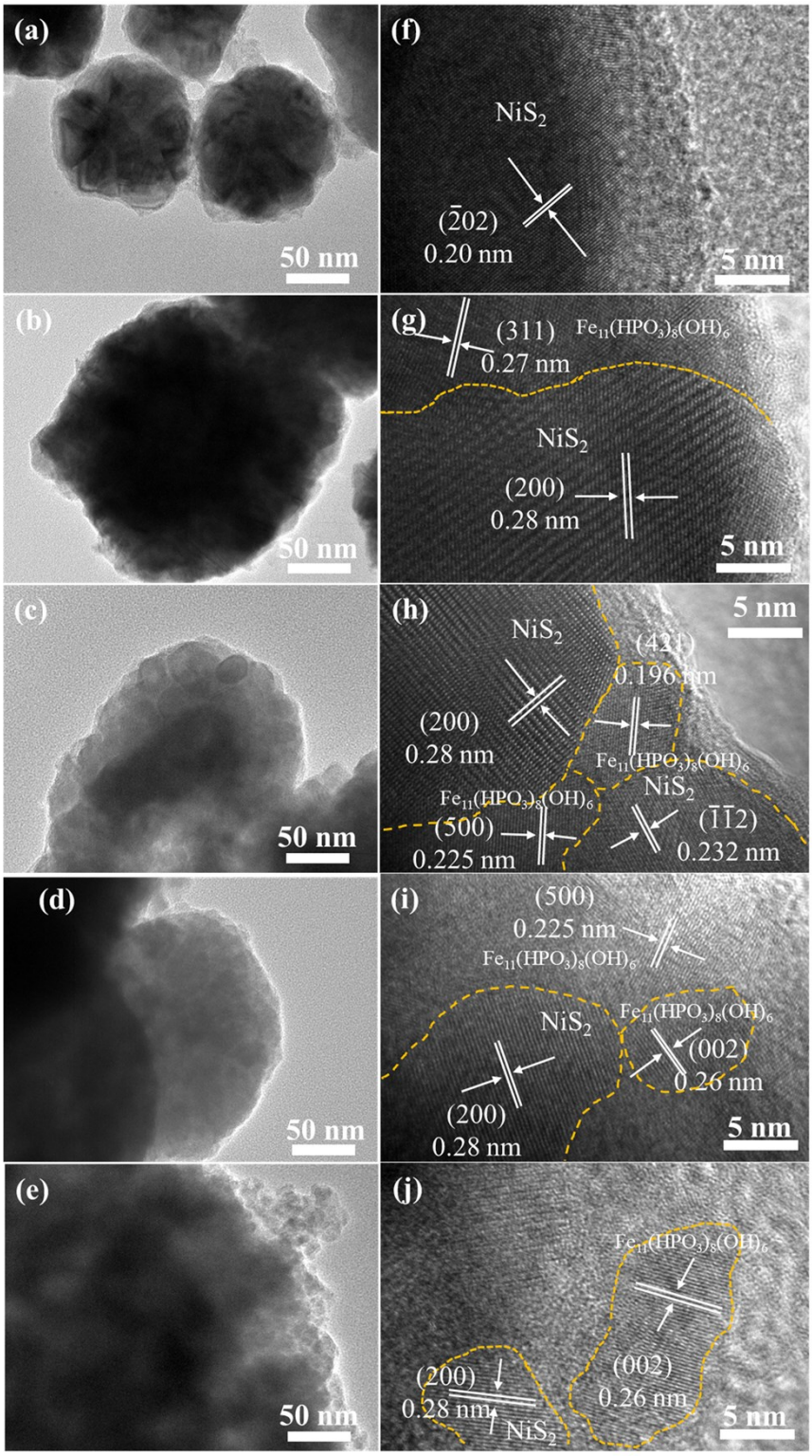

Figure S3. The TEM and HRTEM images of (a, f) pure NiS_2; (b, g) $NiS_2/Fe_{0.2}$-P; (c, h) $NiS_2/Fe_{0.4}$-P; (d, i) $NiS_2/Fe_{0.8}$-P and (e, j) $NiS_2/Fe_{1.0}$-P.

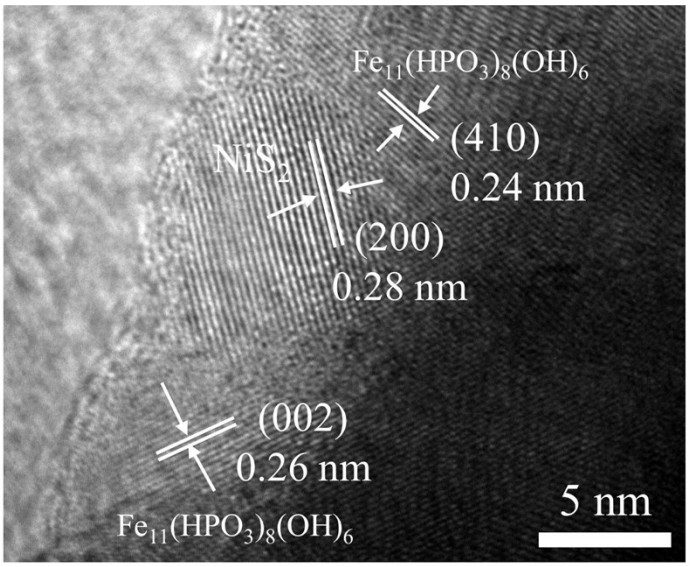

Figure S4. The another HRTEM image of $NiS_2/Fe_{0.4}$-P.

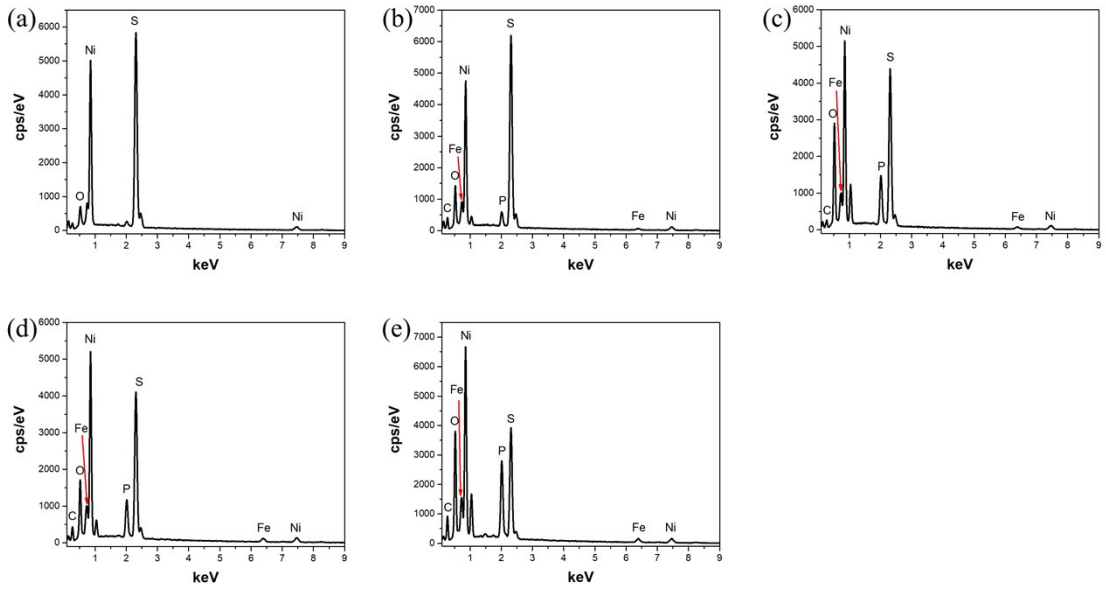

Figure S5. EDS spectra of (a) NiS_2, (b) $NiS_2/Fe_{0.2}$-P, (c) $NiS_2/Fe_{0.4}$-P，(d) $NiS_2/Fe_{0.8}$-P and $NiS_2/Fe_{1.0}$-P.

Table S1. ICP-MS of Ni, Fe, S and P elements from NiS_2/Fe-P ($Fe_{0.2}$, $Fe_{0.4}$, $Fe_{0.8}$ and $Fe_{1.0}$), Ni and S elements from pure NiS_2.

Sample	Element	Content (μg/mL)	Atom%
NiS_2	Ni	14.42	34.5
	S	14.96	65.5
$NiS_2/Fe_{0.2}$-P	Ni	13.98	30.7
	Fe	1.39	3.2
	S	14.87	59.9
	P	1.48	6.2
$NiS_2/Fe_{0.4}$-P	Ni	12.23	29.2
	Fe	2.089	5.3
	S	12.84	56.1
	P	2.08	9.4
$NiS_2/Fe_{0.8}$-P	Ni	11.80	24.1
	Fe	4.49	9.7
	S	12.62	47.2
	P	4.91	19.0
$NiS_2/Fe_{1.0}$-P	Ni	10.64	23.0
	Fe	5.02	11.4
	S	11.55	45.7
	P	4.87	19.9

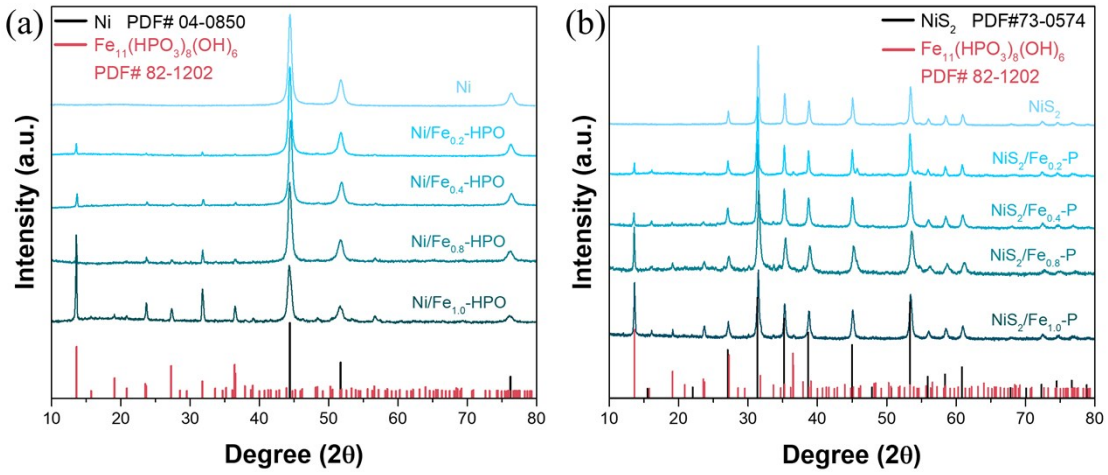

Figure S6. XRD patterns of (a) Ni and all Ni/Fe-HPO; (b) NiS_2 and all NiS_2/Fe-P.

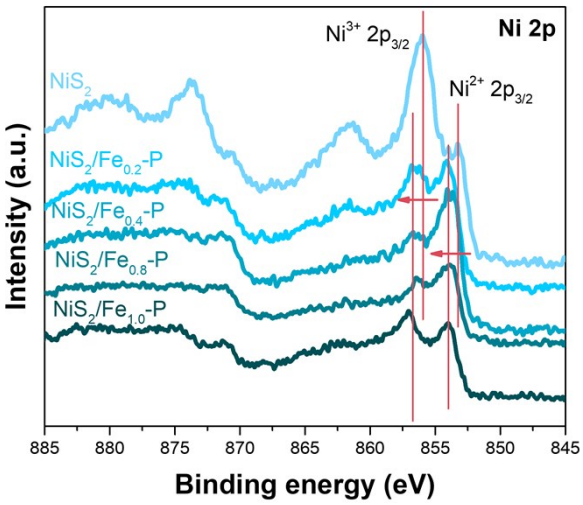

Figure S7. Ni 2p spectra for pure NiS_2 and all NiS_2/Fe-P.

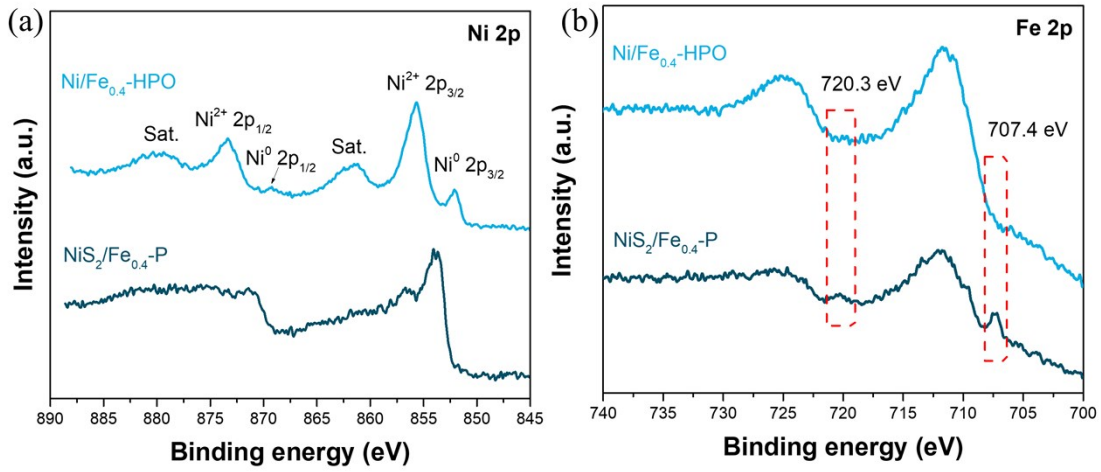

Figure S8. (a) Ni 2p and (b) Fe 2p XPS spectra for Ni/$Fe_{0.4}$-HPO and NiS_2/$Fe_{0.4}$-P.

In the Ni 2p spectrum of Ni/$Fe_{0.4}$-HPO, two peaks located at the binding energy of 852 and 869.6 eV are assigned to the $2p_{3/2}$ and $2p_{1/2}$ of Ni^0. After sulfidation process, the peaks for Ni^0 disappear in the Ni 2p spectrum of NiS_2/$Fe_{0.4}$-P, indicating that the Ni^0 was all transformed to NiS_2. As for Fe 2p spectra, NiS_2/$Fe_{0.4}$-P shows two new peaks at 707.4 and 720.3 eV, which can be ascribed to Fe-P species. It prove that part of $Fe_{11}(HPO_3)_8(OH)_6$ was converted to iron phosphide species during the sulfidation process.

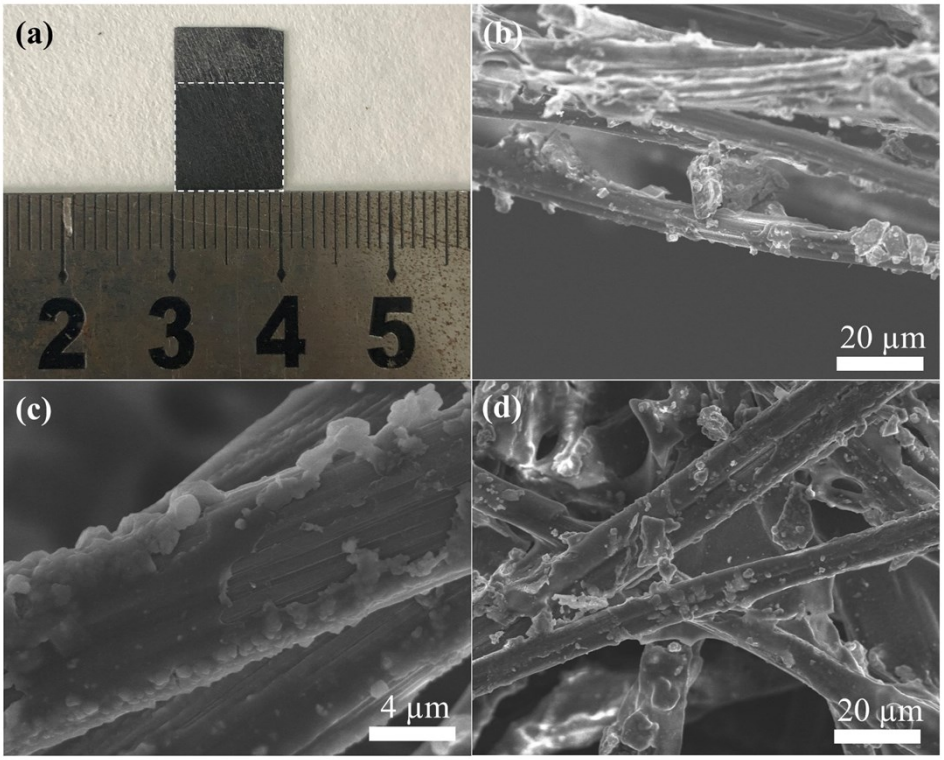

Figure S9. The optical photo (a) and the SEM images of side (b) and top (c,d) surface of the carbon paper with $NiS_2/Fe_{0.4}$-P electrocatalysts loading of ~ 0.98 mg·cm^{-2} used as work electrode.

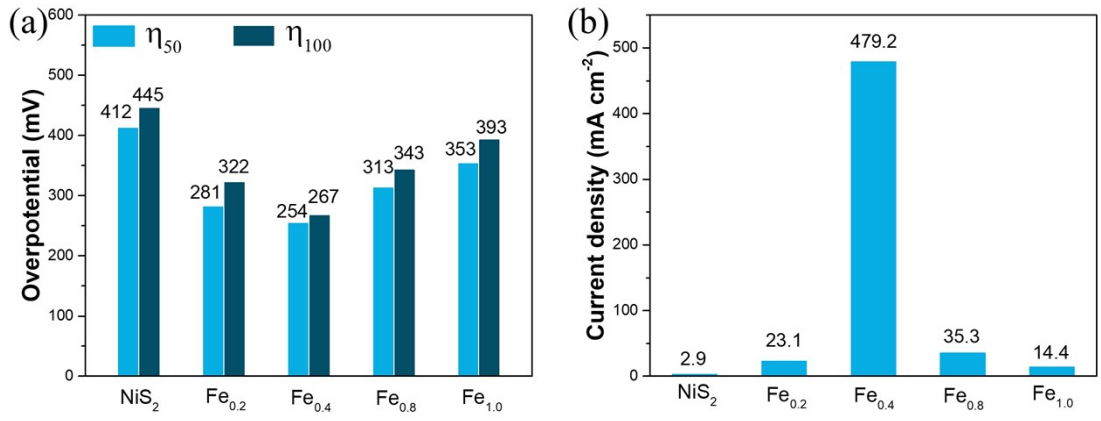

Figure S10. Histogram analysis of (a) overpotential at the current density of 50 and 100 mA·cm^{-2}, (b) current density at the overpotential of 300 mV.

Table S2. Calculation of Faradic efficiency.

Catalyst	***j***/mA·cm^{-2}	***t***/hours	V_{O2}/mL	***FE***/%
$NiS_2/Fe_{0.4}$-P	100	2	40.75	97.5

The Faradic efficiency (FE) of $NiS_2/Fe_{0.4}$-P in 1 M KOH towards OER was calculated as the ratio of experimental and theoretical values of oxygen production, and illustrated as follows:

$$FE = \frac{4 \times F \times n_{O_2}}{I \times t} \times 100\%$$

F is the Faraday constant (96485.33289 C·mol^{-1}), n_{O_2} is the amount of experimentally generated O_2 gas, *I* is the constant current applied and *t* is the reaction time.

Here, the quantity of the experimentally generated O_2 gas was measured by the conventional water-gas displacement method at a constant current density of 100 mA·cm^{-2} for 2 hours using a 1 cm^2 carbon paper electrode, and the volume of O_2 gas collected in this work is 40.75 mL. The theoretically generated O_2 gas was excepted from the charge transfer.

Table S3. Comparison of OER performance for $NiS_2/Fe_{0.4}$-P catalyst with previously reported non-noble metal-based electrocatalysts in alkaline media.

Electrocatalyst	**Substrate**	**Overpotential (η_{10}, mV)**	**Overpotential (η_{100}, mV)**	**Tafel slope (mV·dec^{-1})**	**Ref.**
$NiS_2/Fe_{0.4}$-P nanospheres	Carbon paper	218	268	47.5	**This work**

MoS_2/NiS_2 nanosheets	Carbon cloth	278	393	91.7	*Adv. Sci.* **2019**, 6, 1900246
N-$NiMoO_4/NiS_2$ nanowires/nanosheets	Carbon cloth	267	335	44.3	*Adv. Funct. Mater.* **2019**, 29, 1805298
MoS_2-Ni_3S_2 heteronanorods	Nickle foam	249	~340	57	*ACS Catal.* **2017**, 7, 2357
NiTe/NiS Nanoarrays/nanaodots	Nickle foam	209	257	49	*Adv. Mater.* **2019**, 31, 1900430
Fe_2O_3@Ni_2P/$Ni(PO_3)_2$ nanoparticles	Nickle foam	\	300	48.2	*J. Mater. Chem. A* **2019**, 7, 965
NiFe-LDH nanosheets	Glass carbon	310	\	74	*ACS Sustainable Chem. Eng.* **2019**, 7,4247
Ni_3S_2@MoS_2/FeOOH nanosheets	Carbon cloth	234	282	49	*Appl. Catal. B* **2019**, 244, 1004
Fe-Ni@NC-CNTs	Glassy carbon dish	274	\	45.5	*Angew. Chem.* **2018**, 130, 9059
$Ni_{11}(HPO_3)_8(OH)_6$/NF	Nickle foam	232	362	\	*Energy Environ. Sci.* **2018**, 11, 1287
$Fe_{11.7\%}$-$Co_{11}(HPO_3)_8(OH)_6$	Nickle foam	206	\	47	*Electrochimica Acta* **2020**, 334, 135616
$Co_{11}(HPO_3)_8(OH)_6$/$Co_{11}(PO_3)_8O_6$ core-shell nanowires	Glassy carbon	340	\	60	*Appl. Catal. B-Environ.* **2019**, 259, 118091
hierarchical Ni-Fe LDH	Glassy carbon	280	\	49.4	*Angew. Chem. Int. Ed.* **2018**, 57,172
(Ni-Fe)S_x/$NiFe(OH)_y$ films	Nickle foam	\	290	58	*Appl. Catal. B-Environ.* **2019**,

					246, 337
3D Fe_2O_3@Ni_2P/$Ni(PO_3)_2$/NF	Nickle foam	\	300	48.2	*J. Mater. Chem. A,* **2019**, 7, 965
Fe-Ni_3S_2/NF	Nickle foam	214	249	42	*ACS Catal.* **2018**, 8, 5431

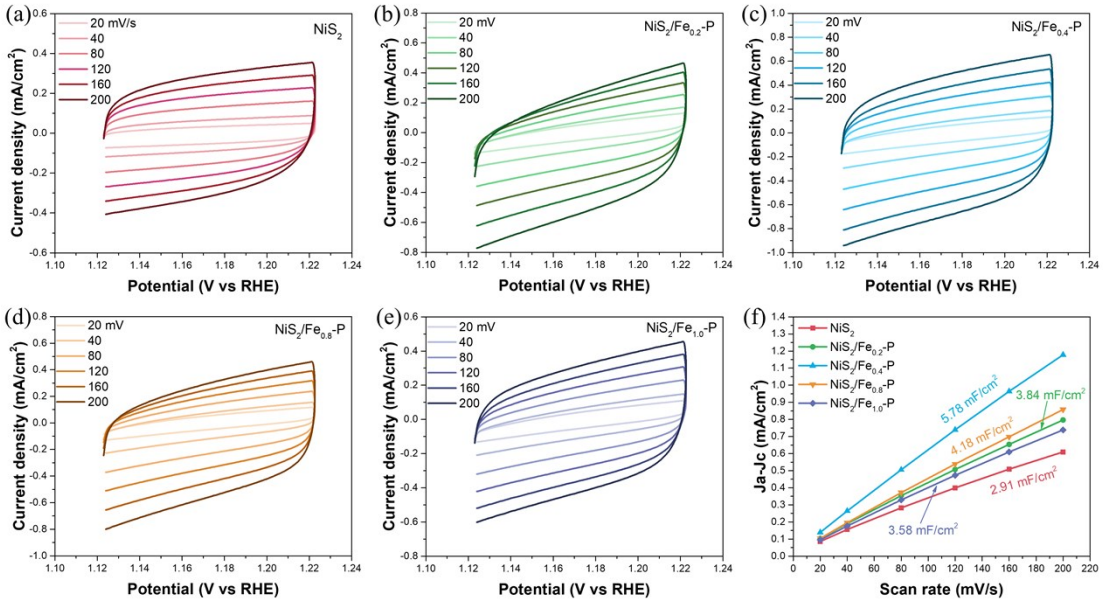

Figure S11. Cyclic voltammogram (CV) curves of (a) NiS_2, (b) $NiS_2/Fe_{0.2}$-P, (c) $NiS_2/Fe_{0.4}$-P, (d) $NiS_2/Fe_{0.8}$-P and (e) $NiS_2/Fe_{1.0}$-P at different scan rates of 20, 40, 80, 120, 160 and 200 mV s^{-1}. (f) The corresponding C_{dl} values of the catalysts.

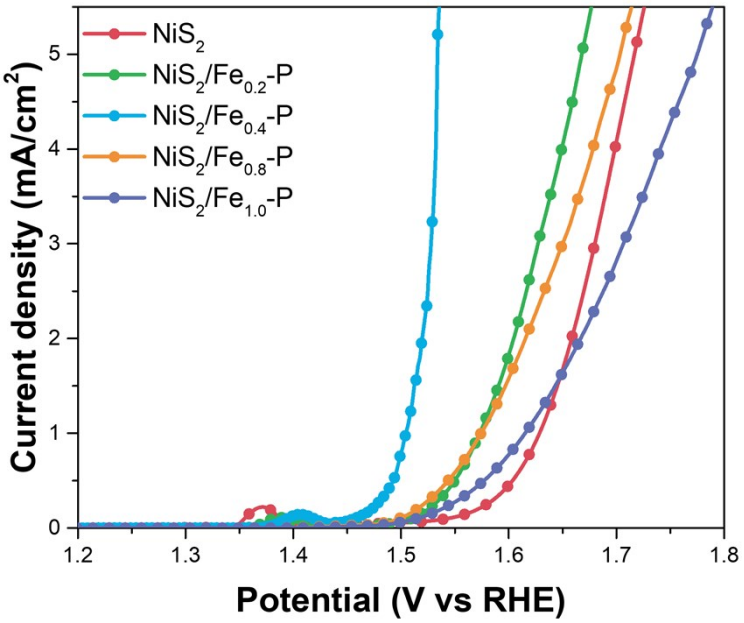

Figure S12. The normalized LSV curves of pure NiS_2 and all NiS_2/Fe-P catalysts.

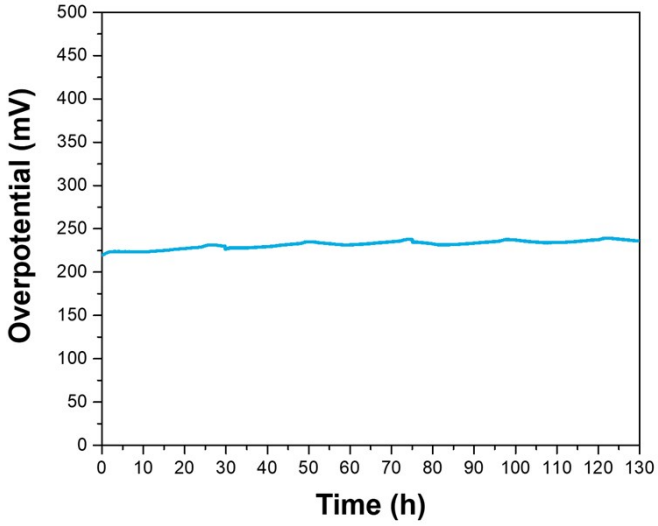

Figure S13. The chronopotentiometry plot of $NiS_2/Fe_{0.4}$-P catalyst for 130 h at the current density of 10 $mA \cdot cm^{-2}$.

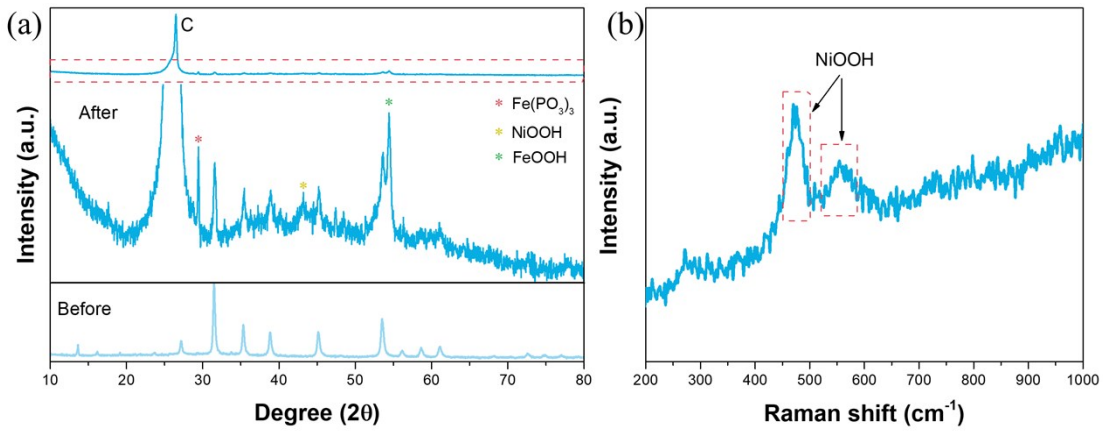

Figure S14. (a) The XRD patterns of $NiS_2/Fe_{0.4}$-P catalyst before and after long-term OER test; (b) The Raman spectrum of $NiS_2/Fe_{0.4}$-P catalyst after long-term OER test.

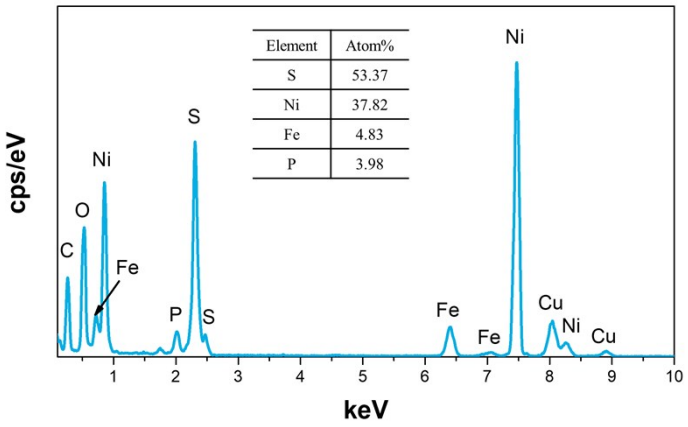

Figure S15. EDS spectrum of $NiS_2/Fe_{0.4}$-P catalyst after long-term OER test.

Table S4. ICP-MS of Ni, Fe, S and P elements from $NiS_2/Fe_{0.4}$-P catalyst after long-term OER test.

Element	Content (μg/mL)	Atom%
Ni	10.78	35.76
Fe	1.296	4.52
S	9.137	55.48
P	0.674	4.24

REFERENCES

(1) McCrory, C.; Jung, S.; Ferrer, I. M.; Chatman, S. M.; Peters, J. C.; Jaramillo, T. F. Benchmarking Hydrogen Evolving Reaction and Oxygen Evolving Reaction Electrocatalysts for Solar Water Splitting Devices. *J. Am. Chem. Soc.* **2015**, *137*, 4347-4357.